

Soft Matter

Accepted Manuscript



This is an *Accepted Manuscript*, which has been through the Royal Society of Chemistry peer review process and has been accepted for publication.

Accepted Manuscripts are published online shortly after acceptance, before technical editing, formatting and proof reading. Using this free service, authors can make their results available to the community, in citable form, before we publish the edited article. We will replace this *Accepted Manuscript* with the edited and formatted *Advance Article* as soon as it is available.

You can find more information about *Accepted Manuscripts* in the [Information for Authors](#).

Please note that technical editing may introduce minor changes to the text and/or graphics, which may alter content. The journal's standard [Terms & Conditions](#) and the [Ethical guidelines](#) still apply. In no event shall the Royal Society of Chemistry be held responsible for any errors or omissions in this *Accepted Manuscript* or any consequences arising from the use of any information it contains.

Swim Stress, Motion, and Deformation of Active Matter: Effect of an External Field

Sho C Takatori^{*a} and John F Brady^a

Received 27th June 2014, Accepted Xth XXXXXXXXXX 20XX

First published on the web Xth XXXXXXXXXX 200X

DOI: 10.1039/b000000x

We analyze the stress, dispersion, and average swimming speed of self-propelled particles subjected to an external field that affects their orientation and speed. The swimming trajectory is governed by a competition between the orienting influence (i.e., taxis) associated with the external (e.g., magnetic, gravitational, thermal, nutrient concentration) field versus the effects that randomize the particle orientations (e.g., rotary Brownian motion and/or an intrinsic tumbling mechanism like the flagella of bacteria). The swimmers' motion is characterized by a mean drift velocity and an effective translational diffusivity that becomes anisotropic in the presence of the orienting field. Since the diffusivity yields information about the micromechanical stress, the anisotropy generated by the external field creates a normal stress difference in the recently developed “swim stress” tensor.[Takatori, Yan, and Brady, *Phys Rev Lett*, 2014.] This property can be exploited in the design of soft, compressible materials in which their size, shape, and motion can be manipulated and tuned by loading the material with active swimmers. Since the swimmers exert different normal stresses in different directions, the material can compress/expand, elongate, and translate depending on the external field strength. Such an active system can be used as nano/micromechanical devices and motors. Analytical solutions are corroborated by Brownian dynamics simulations.

1 Introduction

Understanding the complex dynamic behaviors of a suspension of self-propelled colloidal particles, or “active matter,” has been an important but challenging problem owing to its constituents' ability to generate their own internal stress and drive the system far from equilibrium. This allows intriguing phenomena to arise that otherwise may not take place in a classical equilibrium system, like athermal self-assembly and pattern formation.¹ Recently a new principle was introduced to study such fascinating phenomena—that is, through their self-motion all active matter systems generate an intrinsic “swim stress” that impacts their large-scale collective behavior.² The origin of the swim stress (or pressure) is based upon the notion that all self-propelled bodies must be confined by boundaries to prevent them from swimming away in space. The “swim pressure” is the unique pressure exerted by the swimmers as they bump into the surrounding walls that confine them. The same principle applies to molecular gases that collide into the container walls to exert a pressure or to the osmotic pressure exerted by solute molecules.

In this work we build upon this new perspective to analyze an active matter system subjected to an external field that affects its constituents' swimming orientation and speed. External fields like chemical and thermal gradients and/or

the Earth's magnetic and gravitational fields can cause microorganisms to modify their swimming behavior to facilitate movement to a favorable region. For example, *E. coli* have been known to undergo chemotaxis by preferentially swimming towards (or away from) chemical gradients of nutrients (or toxins).³ Other examples of taxis swimmers include phototactic,⁴ magnetotactic,⁵ and gravitactic⁶ bacteria.

External orienting fields cause the effective translational diffusivity to become anisotropic, which directly implies the existence of normal stress differences. The micromechanical stress in a dilute suspension is given by the first moment of the force, $\sigma = -n\langle xF \rangle$, where n is the number density of particles and the angle brackets denote an ensemble average over all particles and time. The particle position at time t is $x(t) = \int U(t') dt'$, and from the overdamped equation of motion, $\mathbf{0} = -\zeta\mathbf{U}(t) + \mathbf{F}(t)$, we obtain $\sigma = -n\langle xF \rangle = -n\zeta \int \langle \mathbf{U}(t')\mathbf{U}(t) \rangle dt' = -n\zeta\langle \mathbf{D} \rangle$, where ζ is the hydrodynamic drag factor and the time integral of the velocity autocorrelation is the diffusivity of the particle, \mathbf{D} . A particle undergoing any type of random motion therefore exerts a stress and a pressure, $\Pi = -\text{tr}\sigma/3 = n\zeta\mathbf{D}$. This general result applies for Brownian particles where $D_0 = k_B T/\zeta$, leading to the familiar ideal-gas Brownian osmotic pressure $\Pi^B = nk_B T$. Using the swim diffusivity of active particles in the absence of an external field, $\langle \mathbf{D}^{swim} \rangle = U_0^2 \tau_R \mathbf{I}/6$ where U_0 is the swim speed of the active particle and τ_R is the reorientation time due to rotary Brownian motion and/or an intrinsic reori-

^a Division of Chemistry and Chemical Engineering, California Institute of Technology, Pasadena, CA 91125 USA. E-mail: Takatori@caltech.edu

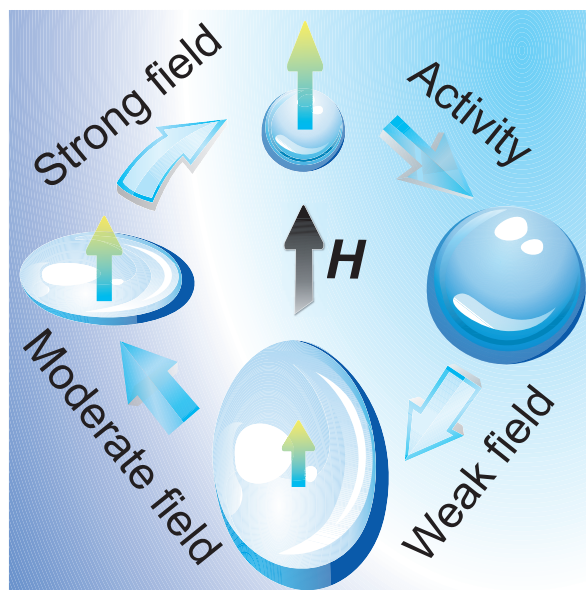


Fig. 1 Schematic of the shape, size, and motion of a soft, compressible gel loaded with light-activated synthetic colloidal particles. When both the light and external field (H) are turned on, the gel translates in the direction of the field (shown by arrows on the gel). The external field strength can be tuned to change the shape, size, and velocity of the gel.

entation mechanism, we obtain the “ideal-gas” swim stress: $\sigma^{swim} = -n\langle \mathbf{x}\mathbf{F}^{swim} \rangle = -n\zeta\langle \mathbf{D}^{swim} \rangle = -n\zeta U_0^2 \tau_R \mathbf{I}/6$, where $\mathbf{F}^{swim} \equiv \zeta \mathbf{U}_0$ is the self-propulsive force of the swimmer.² Although it is clear that an external field may cause the effective diffusivity and hence the swim stress to become anisotropic, how is this normal swim-stress difference generated and what are its implications on the design of novel active soft-matter materials?

To appreciate the importance of normal swim stresses, we discuss an important application of this work in the design of nano/micromechanical devices and motors. Suppose we load a soft, compressible material (e.g., gel polymer network) with light-activated synthetic colloidal particles. In the absence of light, the colloidal particles simply fluctuate due to Brownian motion, and the gel assumes some equilibrium shape as shown on the top of Fig 1. The equilibrium volume of the gel is determined by the balance of the force that drives the polymer to expand and mix with the solvent versus the elastic force that resists the expansion.⁷ When the light is turned on, the colloidal particles become active and exert an additional “ideal-gas” swim pressure, $\Pi^{swim} = -\text{tr}\sigma^{swim}/3 = n\zeta U_0^2 \tau_R/6$, causing the gel to expand isotropically as shown in the sketch on the right. The relative magnitudes of the swim pressure versus the shear modulus of the gel, G , determine whether the gel expands appreciably in the presence of the swim-

mers. In principle the shear modulus of polymer networks can be adjusted to nearly zero. A dilute network of hydrated mucus, which behaves as a non-Newtonian gel, has shear moduli of order $\sim \mathcal{O}(0.1 - 10)Pa$,^{8,9} but here we estimate $G \approx n_c k_B T$ where n_c is the number density of sub-chains in the network (related to the cross-link density).⁷ The energy scale associated with $1\mu m$ swimmers traveling in water with speed $U_0 \sim 10\mu m/s$ and reorienting in time $\tau_R \sim 10s$ is $\zeta U_0^2 \tau_R/6 \approx 4pN \cdot \mu m$. The thermal energy at room temperature is $k_B T \approx 4 \times 10^{-3} pN \cdot \mu m$, meaning that the swimmers’ intrinsic self-propulsion is equivalent to approximately $1000k_B T$. In practice the intrinsic activity of active synthetic colloidal particles can be even larger. The swim pressure makes an appreciable contribution to the overall size of the gel if $G/\Pi^{swim} = n_c k_B T/(n1000k_B T) \lesssim \mathcal{O}(1)$, or when the ratio of the polymer sub-chain density to the active-swimmer density is $n_c/n \lesssim 1000$. The swim pressure exerted at 10% volume fraction of active particles is $\Pi^{swim} = n\zeta U_0^2 \tau_R/6 \approx \mathcal{O}(1)Pa$. For gels with a very small shear modulus, the swim pressure can cause the gel to deform its shape. As the gel expands due to the swim pressure, the concentration of swimmers decreases. The new volume of the gel is determined by the balance of the gel’s expansion forces, the osmotic pressure of the polymer chains, and the swim pressure exerted by the swimmers. Even if the gel does not deform, it can still be translated and steered using the active swimmers.

As we shall see in Section 6, when we then apply a weak external field to the system (gel plus swimmers), the gel reacts in three ways as shown on the bottom of Fig 1: it expands even more due to an increase in the swim pressure; it elongates in the field direction due to a positive normal stress difference (i.e., the swimmers exert different magnitudes of normal stresses in different directions of the bounding gel network); the entire gel translates in the field direction due to the net motion of the active swimmers colliding into the gel network. Upon further increase in the external field strength, the swim pressure decreases and the normal stress difference becomes negative, which causes the gel to shrink in size, translate faster towards the field direction, and assume the shape of a thin disk as shown on the left of Fig 1. When the external field strength is made very high, the normal swim-stress difference and swim pressure vanish, causing the gel to return to its equilibrium shape and size but translate in the field direction.

We can make a simple estimate of the gel speed. If an active particle is tethered to a passive particle then it must drag along the passive particle as it swims. The propulsive force available to the swimmer, $\mathbf{F}^{swim} \equiv \zeta \mathbf{U}_0$, must now balance the combined drag of the swimmer ($-\zeta \mathbf{U}$) and its “cargo,” which is characterized by a Stokes drag coefficient ζ_C . Thus, the velocity of the combined object is $\mathbf{U} = \zeta \mathbf{U}_0/(\zeta_C + \zeta)$. If N swimmers are attached the ve-

locity would now go as $\mathbf{U} = N\zeta\mathbf{U}_0/(\zeta_C + N\zeta)$. The same principle and estimate apply to swimmers confined to a gel. The total propulsive force available is $\mathbf{F} \sim nV_{gel}\zeta\langle\mathbf{u}\rangle$, where V_{gel} is the volume of the gel and $\langle\mathbf{u}\rangle$ is the mean swimmer velocity in the presence of the external field (calculated in Sections 4 and 6). This force must balance the gel and swimmers' drag $\mathbf{F}^{drag} = -(\zeta_{gel} + nV_{gel}\zeta)\mathbf{U}_{gel}$ to give $\mathbf{U}_{gel} \sim nV_{gel}\langle\mathbf{u}\rangle\zeta/\zeta_{gel}(1/(1 + nV_{gel}\zeta/\zeta_{gel}))$. The porosity and geometry of the gel would influence ζ_{gel} , but the drag is proportional to \mathbf{U}_{gel} as in any Stokes-flow problem.

When the external field is turned off, the gel stops translating and an entire cycle is completed as depicted in Fig 1. Here we have assumed that the active particles are confined to the gel and that the fluid (solvent) is able to flow through the gel as needed. Instead of a gel we can also have a membrane, vesicle, fluid sack, or droplet. To ensure that the system is in osmotic balance with the solvent inside the vesicle, the surrounding membrane must be permeable to the solvent. The resistance to motion of the vesicle would now be set by the permeability of the membrane and the propulsive force determined by the number of swimmers contacting the (interior) upstream surface of the vesicle. If we had a vesicle or fluid droplet that is impermeable to the solvent, then the droplet may still deform and may also translate depending on its shape and mechanical properties of its surface or bounding membrane. A rigid object filled with fluid and swimmers would not deform nor translate; the active motion of the swimmers would set up a recirculating flow within the rigid object.

To continue in the design of nano/micromechanical devices and motors, suppose we rotate the external field by 90 degrees. For a moderate external field strength (sketched on the left of Fig 1), the gel reacts differently depending on the relative magnitude of the characteristic angular velocity induced by the external field, Ω_c , and the rate at which we rotate the field, Ω_{ext} . When we rotate the field slowly, $\Omega_{ext}/\Omega_c \ll 1$, the gel maintains its current shape and slowly changes its orientation with the swimmers, tracing an arc and continuing a path along the new field direction, as shown on the top of Fig 2. When we rotate the field quickly, $\Omega_{ext}/\Omega_c \gg 1$, the swimmers respond quickly and begin to swim in the new field direction. In this limit the gel temporarily stops translating because the swimmers do not take any swim steps between their reorientations. After the swimmers change their orientations toward the new field direction, the gel again assumes a disk shape and translates with the swimmers. As illustrated in Figs 1 and 2, by tuning the properties of the gel (or vesicle or drop), the activity of the swimmers, and the strength of the external orienting field, a wide range of controllable motion is possible. It is important to note that if one can measure the effective translational diffusivity of active particles in an orienting field, then the stress is known from the relationship $\sigma = -n\zeta\langle\mathbf{D}\rangle$. We can thus make predictions of the shape and size of the gel based upon

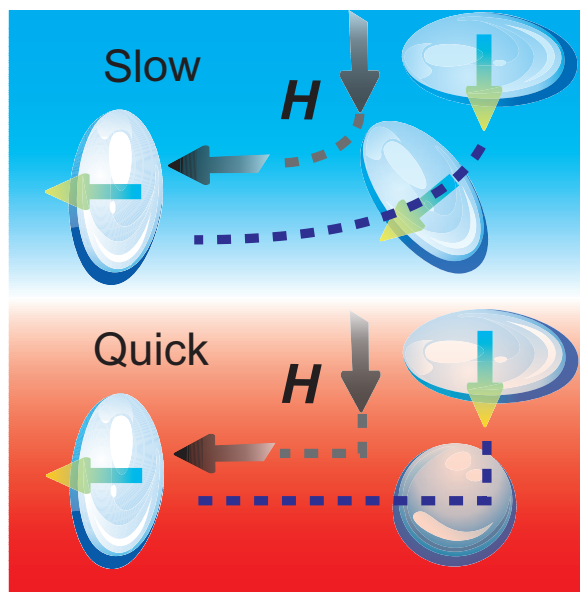


Fig. 2 Schematic of the motion of a soft, compressible gel loaded with active particles when the external field is rotated by 90 degrees. The shape and trajectory of the gel depends on the relative rate of rotation of the field and the strength of the field.

a simple diffusivity measurement of the swimmers.

The motion of a single particle due to an intrinsic swim force and an external force are the same. At higher concentrations or when considering the swimmer's interactions with other bodies or boundaries a distinction must be made—the intrinsic swim mechanism does not generate a long-range $1/r$ Stokes velocity field as does an external force. In our analysis we neglect hydrodynamic interactions among the particles, which would contribute additional terms to the active-particle stress and affect the reorientation time of the particles. It is important to note that the swim stress presented here is distinct and different from the “hydrodynamic stresslet,” which is also a single-particle property but scales as $\sim n\zeta U_0 a$ where a is the particle size.^{10,11} No study to date has studied the effect of an external field on the swim stress of active matter. The ratio of the magnitude of the hydrodynamic stresslet over the swim pressure is the reorientational Péclet number, $Pe_R = U_0 a / \langle D^{swim} \rangle \sim a / (U_0 \tau_R)$, which compares the swimmer size a to its run length $U_0 \tau_R$.² The hydrodynamic contribution to the deformation of soft materials becomes negligible at low Pe_R , the regime in which many synthetic active particles operate.^{12,13}

In this paper we present a micromechanical model that determines the average translational velocity, diffusivity, and swim stress of a suspension of active particles in any external field. Previous studies of the translational diffusivity of Brownian particles have used a generalized Taylor dispersion

method to analyze the behavior when subjected to an external orienting field and/or a homogeneous shear flow.^{14–18} Manela and Frankel¹⁷ analyzed the effective translational diffusivity of dipolar swimmers subjected to a simple shear flow and an external field, and Bearon and coworkers^{19,20} extended the analysis to different flow conditions. Owing to slow numerical convergence, most studies have focused on weak external fields; in practice, however, active particles may be exposed to strong external fields, be it a chemical or thermal gradient field. As shown in this work, strong external fields are interesting because the convective enhancement to the effective translational diffusivity ($\langle D^{swim} \rangle = U_0^2 \tau_R / 6$) vanishes entirely. Furthermore, most studies assume a constant swimming speed of the particles, irrespective of the external field strength. In nature or in the laboratory, the local chemical and thermal environments can affect the swimming speeds of active particles. Indeed, bacteria modulate their swimming speeds when exposed to a thermal²¹ or chemoattractant concentration field.²² We address this problem by allowing the swimmers to modify their speeds based on their instantaneous orientation. Our analytical model is corroborated by Brownian dynamics (BD) simulations.

The balance between the strength of the orienting field and the effects that randomize the particle orientation is characterized by the Langevin parameter, $\chi_R = \Omega_c \tau_R$, where Ω_c is the characteristic angular velocity induced by the external field and τ_R is the reorientation time from rotary Brownian motion and/or an intrinsic reorientation mechanism. Simple dimensional reasoning provides predictions of the effect of the external field on the average swimming speed, effective translational diffusivity, and swim stress. The self-propulsive enhancement to a swimmer's effective translational diffusivity scales as $\langle D^{swim} \rangle \sim L_{eff}^2 / \tau_R$, where L_{eff} is the effective step size. In the absence of an external field $L_{eff} \sim U_0 \tau_R$, giving $\langle D^{swim} \rangle \sim U_0^2 \tau_R$. With the external field in the linear response regime, the change in the effective step size, $\Delta L_{eff} \sim \chi_R U_0 \tau_R$, so the change in swim stress scales as $\Delta \sigma^{swim} = -n \zeta \langle \Delta D^{swim} \rangle \sim -n \zeta (U_0^2 \tau_R) \chi_R^2$. The average velocity along the external field scales as $\langle u_{\parallel} \rangle \sim L_{eff} / \tau_R \sim U_0 \chi_R$, linear in the forcing. The average velocity transverse to the external field is zero for all values of χ_R : $\langle u_{\perp} \rangle = 0$. Thus, $\langle \mathbf{D} \rangle \sim D_0 + U_0^2 \tau_R / 6 (1 + \mathcal{O}(\chi_R^2))$ and $\sigma^{swim} \sim -n \zeta U_0^2 \tau_R / 6 (1 + \mathcal{O}(\chi_R^2))$ and is anisotropic.

For $\chi_R \gg 1$, the external field is so strong that the swimmers spend most of their time oriented along the field. This suggests that the average swimmer velocity is $\langle u_{\parallel} \rangle \sim U_0 (1 - \chi_R^{-1})$; the instantaneous swimmer velocity is the same as the average velocity, minus a small $\mathcal{O}(\chi_R^{-1})$ correction. The effective translational diffusivity depends on the fluctuation of the swimmers' instantaneous speed from the average speed. This gives the effective step size, $L_{eff} \sim (\langle u \rangle - U_0) \tau_R$. Parallel to the external field we thus have $\sigma_{\parallel}^{swim} = -n \zeta \langle D_{\parallel}^{swim} \rangle \sim$

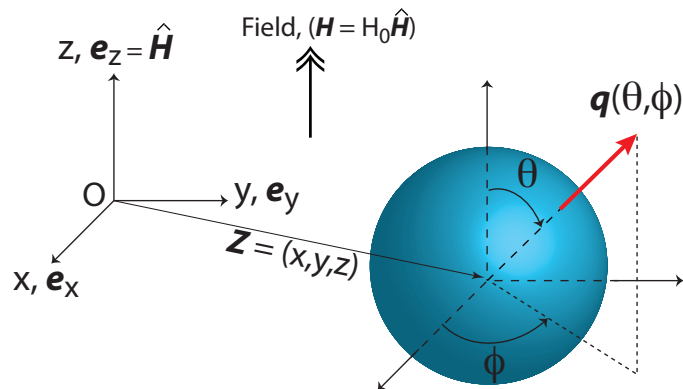


Fig. 3 Definition sketch of an active particle at position \mathbf{z} with orientation \mathbf{q} in an external field, \mathbf{H} .

$-n \zeta U_0^2 \tau_R \chi_R^{-3}$. In the transverse direction, the average velocity is zero so a small fluctuation in an individual swimmer's perpendicular motion affects the dispersion more strongly than small fluctuations along the external field. This suggests that the swimmers' perpendicular velocity decays more slowly, as $u_{\perp} \sim \mathcal{O}(\chi_R^{-1/2})$, giving $\sigma_{\perp}^{swim} = -n \zeta \langle D_{\perp}^{swim} \rangle \sim -n \zeta U_0^2 \tau_R \chi_R^{-2}$. Interestingly, under strong external fields the swim stress and diffusivity tend to zero.

In the next section, we formulate an expression for the average translational flux, from which we deduce the swim stress and the average translational velocity and diffusivity. In section 3, we derive the evolution equations governing the orientation distribution and fluctuation fields. A similar approach has been used to study two-body collisions in nonlinear microrheology,²³ which we extend here into orientation space. In part 4, we consider our first example of swimmers with uniform speeds. We build up our BD simulation framework in section 5 to verify the analytical theory. To obtain a more complete description, in section 6 we allow the swimming speeds to vary with orientation and field strength.

2 Average swimmer motion

We focus on the motion of a single active Brownian particle that swims in a quiescent fluid with an orientation-dependent velocity $\mathbf{u}(\mathbf{q})$, where the unit vector \mathbf{q} specifies its orientation. The swimming velocity can be a result of intrinsic self-propulsion from a living microorganism or an activated synthetic catalytic particle.^{1,24} The particle also undergoes random thermal motion with a translational diffusivity \mathbf{D}_0 , and reorients due to rotary Brownian motion and/or an intrinsic mechanism (e.g., flagella), characterized by a reorientation time τ_R . For torqued swimmers like gravitactic or magnetotactic bacteria, the external field induces an orientation-dependent torque on the particle, $\mathbf{L}^{ext}(\mathbf{q})$. In con-

trast, force and torque-free swimmers like phototactic bacteria or other microorganisms undergoing chemotaxis or thermotaxis may possess an internal mechanism (e.g., biological sensor) to reorient themselves along the field. Our general analysis remains valid whether the reorientation is induced by an external torque or as a result of an intrinsic particle property. The dynamics of an active particle is contained in $P(\mathbf{z}, \mathbf{q}, t | \mathbf{z}_0, \mathbf{q}_0, t_0)$, the conditional probability of finding the particle at position \mathbf{z} and orientation \mathbf{q} at time t , given that it was at \mathbf{z}_0 and \mathbf{q}_0 at time t_0 . This probability density obeys the Smoluchowski equation

$$\frac{\partial P}{\partial t} + \nabla \cdot \mathbf{j}_T + \nabla_q \cdot \mathbf{j}_R = 0, \quad (1)$$

where the translational and rotary fluxes are given by, respectively,

$$\mathbf{j}_T = \mathbf{u}(\mathbf{q})P - \mathbf{D}_0 \cdot \nabla P, \quad (2)$$

$$\mathbf{j}_R = \boldsymbol{\omega}(\mathbf{q})P - \frac{1}{\tau_R} \nabla_q P, \quad (3)$$

where $\boldsymbol{\omega}(\mathbf{q})$ is the orientation-dependent angular velocity of the swimmer, \mathbf{D}_0 is its Brownian translational diffusivity, and ∇ and ∇_q are the physical-space and orientation-space gradient operators, respectively.

We are interested in times $t > \tau_R$ in which all orientations have been sampled. To this end, we follow Zia and Brady²³ and introduce the Fourier transform with respect to position, denoted by $\hat{\cdot}$. Averaging Eqs 1 and 2 over orientation space, we obtain

$$\frac{\partial \hat{n}(\mathbf{k}, t)}{\partial t} + i\mathbf{k} \cdot \langle \hat{\mathbf{j}}_T \rangle = 0, \quad (4)$$

$$\langle \hat{\mathbf{j}}_T \rangle = \oint \mathbf{u} \hat{P} d\mathbf{q} - \mathbf{D}_0 \cdot i\mathbf{k} \hat{n}, \quad (5)$$

where $\hat{n}(\mathbf{k}, t) \equiv \oint \hat{P}(\mathbf{k}, \mathbf{q}, t) d\mathbf{q}$ is the local number density of active particles. We introduce $\hat{P}(\mathbf{k}, \mathbf{q}, t) = g(\mathbf{k}, \mathbf{q}, t) \hat{n}(\mathbf{k}, t)$, and focus on the orientation distribution through the structure function $g(\mathbf{k}, \mathbf{q}, t)$. For the long-time self-diffusion we consider the short wave vector (long length scale) limit²³ and thus expand for small \mathbf{k} : $g(\mathbf{k}, \mathbf{q}, t) = g_0(\mathbf{q}, t) + i\mathbf{k} \cdot \mathbf{d}(\mathbf{q}, t) + \mathcal{O}(\mathbf{k}\mathbf{k})$. The field g_0 is the orientation distribution function, and \mathbf{d} is the probability-weighted displacement or fluctuation of a particle about its mean velocity (i.e., the strength and direction of the swimmer's displacement due to the external field). Readers familiar with Brenner's²⁵ generalized Taylor dispersion theory will notice that g_0 and \mathbf{d} are similar to his P_0^∞ and \mathbf{B} fields, respectively. Introducing this expansion into Eq 5, we obtain the mean particle translational flux:

$$\langle \hat{\mathbf{j}}_T \rangle = \hat{n} [\langle \mathbf{u} \rangle - i\mathbf{k} \cdot \langle \mathbf{D} \rangle], \quad (6)$$

where the average translational velocity and diffusivity are, respectively,

$$\langle \mathbf{u} \rangle = \oint \mathbf{u}(\mathbf{q}) g_0 d\mathbf{q}, \quad (7)$$

$$\langle \mathbf{D} \rangle - \mathbf{D}_0 = \langle \mathbf{D}^{swim} \rangle = \oint (\langle \mathbf{u} \rangle - \mathbf{u}(\mathbf{q})) \mathbf{d} d\mathbf{q}. \quad (8)$$

In Eq 8 the term $\langle \mathbf{u} \rangle$ was inserted to emphasize that it is the velocity fluctuation that generates dispersion.

In the Introduction we derived a direct relationship between the translational diffusivity and the micromechanical stress: $\boldsymbol{\sigma} = -n\zeta \langle \mathbf{D} \rangle$. Substituting Eq 8 into this expression gives the stress generated by the active particle, $\boldsymbol{\sigma} = \boldsymbol{\sigma}^B + \boldsymbol{\sigma}^{swim}$, where we identify the Brownian osmotic stress as $\boldsymbol{\sigma}^B = -n\zeta \mathbf{D}_0 = -nk_B T \mathbf{I}$, and the swim stress as the convective enhancement to the diffusivity (right-hand side of Eq 8):

$$\boldsymbol{\sigma}^{swim} = -n\zeta \oint (\langle \mathbf{u} \rangle - \mathbf{u}(\mathbf{q})) \mathbf{d} d\mathbf{q}. \quad (9)$$

Equations 7 to 9 are the main results we wish to determine. The swim pressure is given by $\Pi^{swim} = -\text{tr} \boldsymbol{\sigma}^{swim} / 3$ and is interpreted as the average normal swim stress (i.e., the confinement forces) necessary to prevent an active body from swimming away in space.²

3 Non-equilibrium orientation and fluctuation fields

We now develop the evolution equations governing the orientation-distribution function g_0 and the fluctuation field \mathbf{d} for use in Eqs 7 to 9. From the Smoluchowski Eq 1, $g(\mathbf{k}, \mathbf{q}, t)$ satisfies

$$\frac{\partial g}{\partial t} + \nabla_q \cdot (\boldsymbol{\omega}(\mathbf{q})g) - \frac{1}{\tau_R} \nabla_q^2 g = g i\mathbf{k} \cdot [\langle \mathbf{u} \rangle - \mathbf{u}(\mathbf{q}) - i\mathbf{k} \cdot (\langle \mathbf{D} \rangle - \mathbf{D}_0)], \quad (10)$$

where g is finite on the unit sphere and is normalized: $\oint g(\mathbf{k}, \mathbf{q}, t) d\mathbf{q} = 1$.

To proceed we need a form of $\boldsymbol{\omega}(\mathbf{q})$, the rotary velocity that reorients the biased swimmer along the external field or gradient, \mathbf{H} . For force and torque-free swimmers, like microorganisms undergoing phototaxis, chemotaxis, and/or thermotaxis, we assume that they possess an intrinsic mechanism (e.g., biological sensor) to reorient themselves along \mathbf{H} . A simple expression for the rotary velocity that models this behavior is $\boldsymbol{\omega}(\mathbf{q}) = \Omega_c \mathbf{q} \times \hat{\mathbf{H}}$, where Ω_c is the magnitude of the angular velocity and $\hat{\mathbf{H}}$ is the unit vector along the field. This expression implies that the swimmer attains the maximum rotary velocity when $\mathbf{q} \perp \hat{\mathbf{H}}$ and zero rotary velocity

when $\mathbf{q} \parallel \hat{\mathbf{H}}$. Another common class of swimmers, like magnetotactic or gravitactic bacteria, reorient themselves owing to a torque induced by the external field, $\boldsymbol{\omega}(\mathbf{q}) = \mathbf{M}_R \cdot \mathbf{L}^{ext}$, where \mathbf{M}_R is the rotary mobility tensor. Following Brenner and Condiff,²⁶ one can show that this leads to the same expression as that of the torque-free swimmers. This implies that the detailed reorientation mechanism is unimportant, and both types of swimmers can be modeled with the same expression for the rotary velocity. When analyzing the motion of a single particle, there is no distinction between rotation caused by an external torque and motion arising inherently from the swimmer.

The equations are made dimensionless by scaling $\mathbf{u} \sim U_0$, $\boldsymbol{\omega}(\mathbf{q}) \sim \Omega_c$, and $\mathbf{d} \sim U_0\tau_R$. Using the small- \mathbf{k} expansion and considering a spherical particle with a constant, isotropic Brownian diffusivity, the steady-state orientation distribution function satisfies a convection-diffusion equation:

$$\nabla_q^2 g_0 - \chi_R \nabla_q \cdot [(\mathbf{q} \times \hat{\mathbf{H}})g_0] = 0, \quad (11)$$

with $\oint g_0 d\mathbf{q} = 1$, and $\chi_R \equiv \Omega_c\tau_R$ is the Langevin parameter. The \mathbf{d} -field satisfies a similar equation, but is forced by deviations from the mean velocity:

$$\nabla_q^2 \mathbf{d} - \chi_R \nabla_q \cdot [(\mathbf{q} \times \hat{\mathbf{H}})\mathbf{d}] = -g_0 (\langle \mathbf{u} \rangle - \mathbf{u}(\mathbf{q})). \quad (12)$$

4 Uniform swimming velocity

In this section, we assume all particles have the nondimensional swim velocity $\mathbf{u}(\mathbf{q}) = \mathbf{q}$. We shall see in section 6 that allowing the speed to change with orientation leads to additional interesting dispersive effects. Equations 11 and 12 have exact analytical solutions, but we first consider the limiting behaviors at low and high χ_R .

4.1 $\chi_R \ll 1$ limit

As shown in Appendix A, we apply a regular perturbation to obtain $g_0(\mathbf{q}) = 1/(4\pi) + \hat{\mathbf{H}} \cdot \mathbf{P}_1(\mathbf{q})\chi_R/(4\pi) + \hat{\mathbf{H}}\hat{\mathbf{H}} : \mathbf{P}_2(\mathbf{q})\chi_R^2/(12\pi) + \mathcal{O}(\chi_R^3)$, where $\mathbf{P}_n(\mathbf{q})$ are the n^{th} -order tensor surface spherical harmonics.²⁷ This is identical to Almog and Frankel's¹⁵ result who considered the sedimentation of axisymmetric non-centrosymmetric particles by gravity. Whether the orienting torque is caused by shape-dependent gravitational settling or from dipole-induced alignment, the orientation distribution is the same.

Substituting this solution into Eq 7, the average translational velocity of the swimmers at low χ_R is

$$\langle \mathbf{u} \rangle = \frac{1}{3}\chi_R \hat{\mathbf{H}} + \mathcal{O}(\chi_R^3). \quad (13)$$

The average velocity increases linearly with χ_R , as predicted from simple scaling arguments. As $\chi_R \rightarrow 0$ the orientation

distribution becomes uniform, resulting in no net swimming speed.

To obtain a leading-order correction in the swim stress and translational diffusivity, we must proceed to the $\mathcal{O}(\chi_R^2)$ \mathbf{d} -field problem. Substituting the \mathbf{d} -field solution (see Appendix A) into Eqs 8 and 9, we obtain the swim diffusivity and stress for $\chi_R \ll 1$:

$$\boldsymbol{\sigma}^{swim} = -n\zeta \langle \mathbf{D}^{swim} \rangle = -\frac{n\zeta U_0^2 \tau_R}{6} \left[\mathbf{I} - \frac{6}{5}\chi_R^2 \left(\frac{7}{27} \hat{\mathbf{H}}\hat{\mathbf{H}} + \frac{1}{8} (\mathbf{I} - \hat{\mathbf{H}}\hat{\mathbf{H}}) \right) \right] + \mathcal{O}(\chi_R^4). \quad (14)$$

We have adopted the transversely isotropic form, where $\hat{\mathbf{H}}\hat{\mathbf{H}}$ and $\mathbf{I} - \hat{\mathbf{H}}\hat{\mathbf{H}}$ correspond to the parallel and perpendicular components relative to the field direction, respectively. As $\chi_R \rightarrow 0$ we recover the ‘‘ideal-gas’’ swim pressure, $\Pi^{swim} = n\zeta U_0^2 \tau_R/6$.² The first effect of the external field appears at $\mathcal{O}(\chi_R^2)$, in agreement with our scaling arguments in the Introduction. Notice that the external field causes a decrease in the translational diffusivity, in contrast to the increase seen in the sedimentation problem.¹⁵ The dispersion decreases here because the particles now swim collectively toward $\hat{\mathbf{H}}$, reducing their tendency to take random swim steps.

4.2 $\chi_R \gg 1$ limit

A singular perturbation scheme is required for $\chi_R \gg 1$ because the problem separates into an outer and inner region. Near $\mu \equiv \hat{\mathbf{H}} \cdot \mathbf{q} \approx 1$ there is an orientation-space boundary layer and the angular coordinate is rescaled as $\hat{\mu} = (1 - \mu)\chi_R \sim \mathcal{O}(1)$. To leading order, g_0 and \mathbf{d} are zero in the outer region because the orientation of the swimmer is confined to a $1/\chi_R$ -thick ‘‘cone’’ around $\mu \approx 1$. As shown in Appendix B, the leading-order boundary-layer solution to Eq 11 is $g_0(\hat{\mu}; \chi_R) = \chi_R e^{-\hat{\mu}}/(2\pi) + \mathcal{O}(1)$. As $\chi_R \rightarrow \infty$, the orientation distribution approaches a delta-function peaked at $\hat{\mu} = 0$, confining the swimming trajectory to a narrow ‘‘cone’’ about the field direction. From Eq 7, the average translational velocity is $\langle \mathbf{u} \rangle = (1 - \chi_R^{-1}) \hat{\mathbf{H}}$. To leading order, all swimmers move along the field direction, $\hat{\mathbf{H}}$, at the same speed, U_0 .

The \mathbf{d} -field problem is resolved into a direction parallel (d_{\parallel}) and perpendicular (d_{\perp}) to the external field. The swim diffusivity and stress for $\chi_R \gg 1$ are

$$\boldsymbol{\sigma}^{swim} = -n\zeta \langle \mathbf{D}^{swim} \rangle = -n\zeta U_0^2 \tau_R \left[\frac{1}{2}\chi_R^{-3} \hat{\mathbf{H}}\hat{\mathbf{H}} + \chi_R^{-2} (\mathbf{I} - \hat{\mathbf{H}}\hat{\mathbf{H}}) \right]. \quad (15)$$

As $\chi_R \rightarrow \infty$, the swim stress vanishes entirely, including the “ideal-gas” pressure $\Pi^{swim} = n\zeta U_0^2 \tau_R / 6$ that was present at low χ_R (see Eq 14). Since all particles are oriented along a $1/\chi_R$ -thick “cone” about the field, each particle swims at the same velocity U_0 towards the same direction, resulting in a vanishingly small dispersion. Since it is the random diffusional motion of a particle that gives rise to a swim pressure, $\Pi^{swim} = n\zeta \text{tr}\langle \mathbf{D}^{swim} \rangle / 3$, a small diffusivity results in a small swim pressure. Another way to understand this is to suppose that the bounding walls in a simulation cell were translating with the average particle velocity, $\langle \mathbf{u} \rangle$. As $\chi_R \rightarrow \infty$, all particles are swimming with the same speed in the same direction so no confinement pressure is required to contain the particles inside the simulation cell.²

4.3 Exact solution for arbitrary χ_R

As given in Appendix C, the solution to Eq 11 for arbitrary χ_R is

$$g_0(\mu; \chi_R) = \frac{\chi_R}{4\pi \sinh \chi_R} e^{\mu \chi_R}, \quad (16)$$

where $\mu \equiv \hat{\mathbf{H}} \cdot \mathbf{q}$ as before in the domain $-1 \leq \mu \leq 1$. From Eq 7, the average translational velocity for arbitrary χ_R is

$$\langle \mathbf{u} \rangle = (\coth \chi_R - \chi_R^{-1}) \hat{\mathbf{H}} \equiv \mathcal{L}(\chi_R) \hat{\mathbf{H}}, \quad (17)$$

where $\mathcal{L}(\chi_R)$ is the Langevin function. As expected, the average perpendicular velocity is zero for all χ_R . We resolve the corresponding displacement field in Eq 12 into the parallel and perpendicular directions. As shown in Appendix C, the parallel direction has an exact solution. In the perpendicular direction, we expand our solution as a series of associated Legendre polynomials. Finally, the effective translational diffusivity and swim stress are obtained from Eqs 8 and 9.

5 Brownian dynamics (BD) simulations

The motion of active particles in an external field can also be analyzed via BD simulations. The system follows the N -particle Langevin equations: $\mathbf{0} = -\zeta(\mathbf{U} - \mathbf{U}_0) + \mathbf{F}^B$ and $\mathbf{0} = -\zeta_R \mathbf{\Omega} + \mathbf{L}^{ext} + \mathbf{L}^R$, where \mathbf{U} and $\mathbf{\Omega}$ are the translational and angular velocities, $\mathbf{F}^{swim} \equiv \zeta \mathbf{U}_0$ is the self-propulsive force, \mathbf{F}^B is the Brownian force, ζ_R is the hydrodynamic resistance coupling angular velocity to torque, and \mathbf{L}^{ext} and \mathbf{L}^R are the torques induced by the external field and rotary Brownian motion and/or an intrinsic reorientation mechanism, respectively. The left-hand sides are zero because inertia is negligible for colloidal dispersions.

The Brownian force and reorientation torque have the white noise statistics $\overline{\mathbf{F}^B} = \mathbf{0}$, $\overline{\mathbf{F}^B(0)\mathbf{F}^B(t)} = 2k_B T \zeta \delta(t) \mathbf{I}$, $\overline{\mathbf{L}^R} = \mathbf{0}$, and $\overline{\mathbf{L}^R(0)\mathbf{L}^R(t)} = 2\zeta_R^2 \delta(t) \mathbf{I} / \tau_R$. Particle orientations were updated by relating $\mathbf{\Omega}$ to the instantaneous orientation \mathbf{q} .²⁸ We varied the Langevin parameter χ_R and analyzed

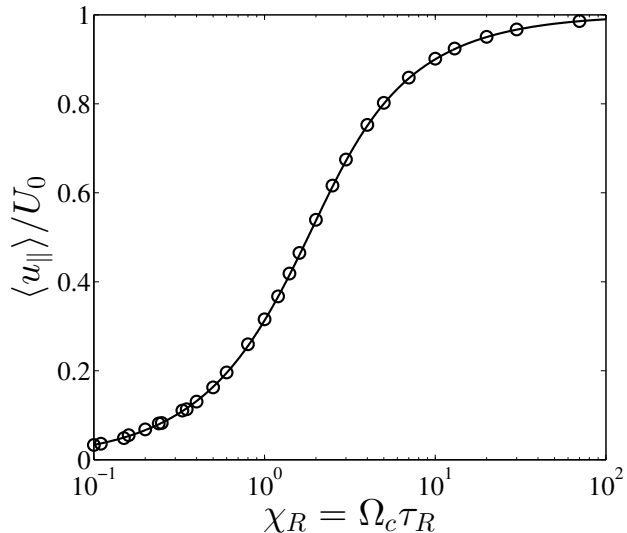


Fig. 4 Average translational velocity along the external field as a function of χ_R . The solid curve is the exact analytical solution, and the circles are data from Brownian dynamics (BD) simulations.

the motion of a single active particle for over 4000 realizations and for at least $100\tau_R$ time.

The average translational velocity and diffusivity are given by $\langle \mathbf{u} \rangle = d\langle \mathbf{x} \rangle / dt$ and $\langle \mathbf{D} \rangle = \lim_{t \rightarrow \infty} d\langle \mathbf{x}' \mathbf{x}' \rangle / (2dt)$, where $\mathbf{x}' = \mathbf{x} - \langle \mathbf{u} \rangle \Delta t$ is the displacement of the swimmer from the mean motion. The swim stress was computed from $\boldsymbol{\sigma}^{swim} = -n\zeta \langle \mathbf{x}' \mathbf{F}^{swim'} \rangle$, where $\mathbf{F}^{swim'} = \mathbf{F}^{swim} - \langle \mathbf{F}^{swim} \rangle$. The average swim force over all realizations, $\langle \mathbf{F}^{swim} \rangle$, must be subtracted to account for the drift velocity of the particles caused by the external field.

5.1 Results

Both the asymptotic and exact solutions of the Smoluchowski equation and BD simulation results are presented here together. Figure 4 shows the nondimensional average swimmer velocity along the external field direction as a function of χ_R . The average velocity increases linearly following Eq 13 for low χ_R , and approaches 1 as $\chi_R \rightarrow \infty$. There is no average speed transverse to the external field.

In the BD simulations, the swim stress was computed using two methods. One approach is to use the definition of the swim stress, $\boldsymbol{\sigma}^{swim} = -n\langle \mathbf{x}' \mathbf{F}^{swim'} \rangle$ (shown in circles in Fig 5). The alternative method is to first calculate the long-time self diffusivity of an active particle and then obtain the swim stress using the relationship $\boldsymbol{\sigma}^{swim} = -n\zeta \langle \mathbf{D}^{swim} \rangle$ (shown in squares). The two methods give identical results, verifying that the stress is indeed directly related to the diffusivity, $\boldsymbol{\sigma} = -n\zeta \langle \mathbf{D} \rangle$. Here we present results for the stress,

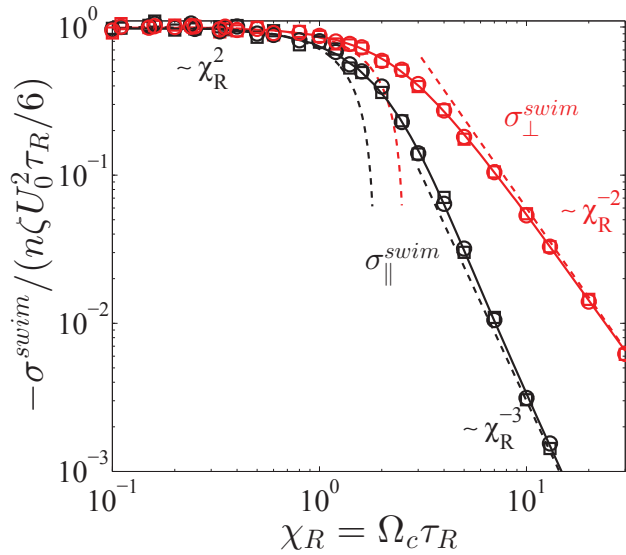


Fig. 5 The swim stress in the parallel (in black) and perpendicular (in red) directions as a function of χ_R , computed in the simulations from $\sigma^{swim} = -n\langle \mathbf{x}' \mathbf{F}^{swim'} \rangle$ (in circles) and also from first obtaining the effective translational diffusivity and then using $\sigma^{swim} = -n\zeta \langle \mathbf{D}^{swim} \rangle$ (in squares). The solid and dashed curves are the exact and asymptotic analytical solutions, respectively.

but the effective translational diffusivity can be obtained by simply dividing the stress by $-n\zeta$.

For $\chi_R \ll 1$, the swim stress reduces to the ideal-gas swim pressure.² The swim stress then decreases as $\sim \mathcal{O}(\chi_R^2)$ following Eq 14. At intermediate values of χ_R (≈ 2), the curves decline as $\sim \mathcal{O}(\chi_R^{-1})$, which means that the dispersion is controlled by convective rotation, i.e., $\sigma^{swim} \sim -n\zeta U_0^2 \tau_R \chi_R^{-1} \sim -n\zeta U_0^2 / \Omega_c$. The diffusivity continues to decay at high χ_R following Eq 15. An interesting feature at high χ_R is the faster decay of $\sigma_{\parallel}^{swim} \sim \mathcal{O}(\chi_R^{-3})$ than $\sigma_{\perp}^{swim} \sim \mathcal{O}(\chi_R^{-2})$. This can be explained by considering the driving force for dispersion, $\Delta \mathbf{u} = \langle \mathbf{u} \rangle - \mathbf{u}(\mathbf{q})$. Gradients in $\Delta \mathbf{u}$ determine the driving force for dispersion: $d\Delta u_{\parallel} / d\hat{\mu} \sim \chi_R^{-1}$ and $d\Delta u_{\perp} / d\hat{\mu} \sim \chi_R^{-1/2} \hat{\mu}^{-1/2}$. The parallel direction has a small driving force for all $\hat{\mu}$ because an individual particle's instantaneous velocity is the same as the mean, $\langle u_{\parallel} \rangle$. A very large fluctuation is required to generate an appreciable contribution to the parallel diffusivity. In contrast, the gradient is maximized at $\hat{\mu} = 0$ in the perpendicular direction because the mean transverse velocity is zero. A small fluctuation in the perpendicular direction contributes more to the dispersion than in the parallel direction, so $\sigma_{\parallel}^{swim}$ decays faster than does σ_{\perp}^{swim} .

Figure 5 shows that the swim stress tensor is anisotropic, which allows us to identify the first normal swim-stress difference: $N_1 = \sigma_{\parallel}^{swim} - \sigma_{\perp}^{swim}$. Remarkably, this normal

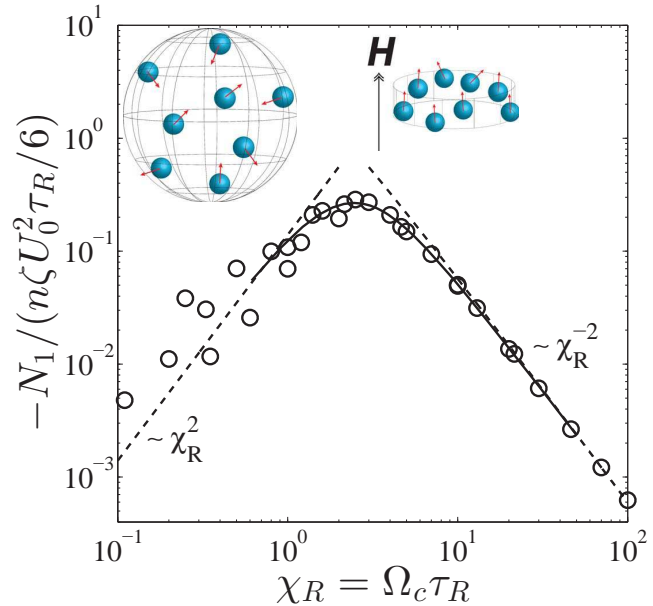


Fig. 6 The first normal swim-stress difference, $N_1 = \sigma_{\parallel}^{swim} - \sigma_{\perp}^{swim}$, as a function of χ_R . The circles are results from BD simulations, and the solid and dashed curves are the exact and asymptotic analytical solutions, respectively. The illustration shows an instantaneous configuration of the swimmers under a weak (sketch on left) and moderate (on right) external field.

swim-stress difference is a *single-particle* property that arises uniquely from the biased motion of an active particle. As shown in Fig 6, N_1 goes to zero for $\chi_R \rightarrow 0$ since the swim stress tensor becomes isotropic. It also goes to zero for $\chi_R \rightarrow \infty$ because the swim stress decays to zero in both the parallel and perpendicular directions (see Eq 15). It reaches a maximum at intermediate values of χ_R owing to the rapid decay of the swim stress in the parallel direction ($\sigma_{\parallel}^{swim} \sim \mathcal{O}(\chi_R^{-3})$). Due to axisymmetry the second normal swim-stress difference is zero for all χ_R .

An anisotropic σ^{swim} means that the confining force required to contain the swimmers by the bounding walls would be different in the parallel and perpendicular directions. The swim pressure represents the average of the normal swim stresses (i.e., confinement pressure) exerted on the bounding walls: $\Pi^{swim} = -\text{tr}\sigma^{swim}/3$.² As shown in Fig 7, the swim pressure approaches the “ideal-gas” value as $\chi_R \rightarrow 0$: $\Pi^{swim} = n\zeta U_0^2 \tau_R / 6$. At higher χ_R , the swim pressure decreases since the external field confines the swimming trajectories along the field direction, reducing the confinement pressure on the surrounding walls.

Since normal stress differences indicate how a soft material might elongate or shrink, results from Figs 6 and 7 can be exploited in the design of various novel active soft materials. Using the results of this section we can now describe how a

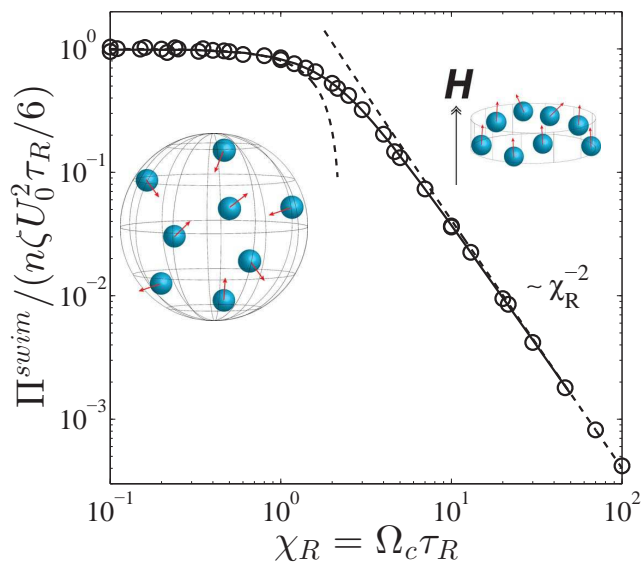


Fig. 7 The swim pressure, $\Pi^{swim} = -\text{tr}\sigma^{swim}/3$, as a function of χ_R . The circles are results from BD simulations, and the solid and dashed curves are the exact and asymptotic analytical solutions, respectively. The illustration shows an instantaneous configuration of the swimmers under a weak (sketch on left) and moderate (on right) external field.

polymer network (e.g., a gel) loaded with active particles with uniform swim speeds behaves in the presence of an external field. In the absence of the external field, the active particles exert an equal magnitude of normal stress in all directions of the gel, namely $\sigma^{swim} = -n\zeta U_0^2 \tau_R \mathbf{I}/6$. Upon turning on the external field, the gel shrinks due to the decrease in swim pressure (see Fig 7), assumes the shape of a thin 3D disk due to the negative normal stress difference (see Fig 6), and the gel translates due to the average velocity of the swimmers (see Fig 4). Such a device can be used as a mechanical device/motor where its shape, size, and motion can be carefully tuned by an external field. The gel behavior discussed in the Introduction (Fig 1) is for non-uniform swim speeds of the particles, which we discuss in Section 6. It is important to note that if one can measure the effective translational diffusivity of active particles in an orienting field, then the stress is known from the relationship $\sigma = -n\zeta\langle\mathbf{D}\rangle$. We can thus make predictions of the shape and size of the gel based upon a simple diffusivity measurement of the swimmers.

6 Nonuniform swimming velocity

The swimming speeds of bacteria have been shown to change when exposed to chemical²² and thermal²¹ gradients. To this end, we now consider the effects of nonuniform swimming speeds on the swim stress and the average translational ve-

locity and diffusivity. Specifically, we allow the swimmers' speed to vary with their orientation relative to the external field, $\mathbf{q} \cdot \mathbf{H}$. Consider the swimming velocity

$$\mathbf{u}(\mathbf{q}) = \mathbf{q} \left(1 + u'(\alpha H_0 \hat{\mathbf{H}} \cdot \mathbf{q}) \right), \quad (18)$$

where $u'(\alpha H_0 \hat{\mathbf{H}} \cdot \mathbf{q})$ is a dimensionless perturbed velocity relative to the uniform speed, U_0 . We introduce α as an intrinsic particle property relating the external field strength, H_0 , to the translational velocity.

The g_0 solution is identical to Eq 16 since the orientation distribution is independent of $\mathbf{u}(\mathbf{q})$. However, the \mathbf{d} -field differs because the driving force $\Delta\mathbf{u} = \langle\mathbf{u}\rangle - \mathbf{u}(\mathbf{q})$ is different. Equation 12 now becomes

$$\nabla_q^2 \mathbf{d} - \chi_R \nabla_q \cdot \left[\left(\mathbf{q} \times \hat{\mathbf{H}} \right) \mathbf{d} \right] = -g_0 \left[\langle\mathbf{u}\rangle - \mathbf{q} \left(1 + u'(\alpha H_0 \hat{\mathbf{H}} \cdot \mathbf{q}) \right) \right], \quad (19)$$

where

$$\langle\mathbf{u}\rangle = \oint g_0 \left[\mathbf{q} \left(1 + u'(\alpha H_0 \hat{\mathbf{H}} \cdot \mathbf{q}) \right) \right] d\mathbf{q}. \quad (20)$$

The swim diffusivity and stress become

$$\sigma^{swim} = -n\zeta\langle\mathbf{D}^{swim}\rangle = -n\zeta U_0^2 \tau_R \oint \left[\langle\mathbf{u}\rangle - \mathbf{q} \left(1 + u'(\alpha H_0 \hat{\mathbf{H}} \cdot \mathbf{q}) \right) \right] \mathbf{d} d\mathbf{q}. \quad (21)$$

Equations 19-21 are the only changes required to account for nonuniform swimming speeds. With a choice of $u'(\alpha H_0 \hat{\mathbf{H}} \cdot \mathbf{q})$, the problem statement is complete. Here we consider a linear relationship for the velocity perturbation: $u'(\alpha H_0 \hat{\mathbf{H}} \cdot \mathbf{q}) = \alpha H_0 \hat{\mathbf{H}} \cdot \mathbf{q}$. A swimmer's velocity is now

$$\mathbf{u}(\mathbf{q}) = \mathbf{q} \left[1 + \alpha H_0 (\mathbf{q} \cdot \hat{\mathbf{H}}) \right], \quad (22)$$

which may be a more complete description than the uniform-speed case considered earlier. When oriented along $\hat{\mathbf{H}}$, the swimmer increases its speed, and when oriented antiparallel to $\hat{\mathbf{H}}$, it decreases its speed.

Substituting Eqs 22 and 16 into Eq 20, the average velocity is

$$\langle\mathbf{u}\rangle = \hat{\mathbf{H}} \left[\coth \chi_R - \chi_R^{-1} + \alpha H_0 \left(1 - 2\chi_R^{-1} \coth \chi_R + 2\chi_R^{-2} \right) \right]. \quad (23)$$

Comparing with Eq 17, we see that the average velocity increases by the last term in parentheses on the right-hand side. At low χ_R , the mean velocity of the swimmers is

$$\langle\mathbf{u}\rangle = \hat{\mathbf{H}} \left(\frac{1}{3} \alpha H_0 + \frac{1}{3} \chi_R + \frac{2}{45} \alpha H_0 \chi_R^2 + \mathcal{O}(\chi_R^3) \right). \quad (24)$$

The first term on the right-hand side represents a mean drift velocity arising from the perturbed velocity. At high χ_R , the swimmers are strongly oriented along the field direction, so the average velocity approaches $U_0(1 + \alpha H_0)$ following Eq 22.

An analytic solution of Eq 19 for arbitrary χ_R and αH_0 is available in Appendix D, but here we analyze the behavior at low and high χ_R . At low χ_R , a regular perturbation scheme gives the swim stress $\sigma^{swim} = -n\zeta \left[\langle D_{\parallel}^{swim} \rangle \hat{\mathbf{H}} \hat{\mathbf{H}} + \langle D_{\perp}^{swim} \rangle (\mathbf{I} - \hat{\mathbf{H}} \hat{\mathbf{H}}) \right]$, where

$$\langle D_{\parallel}^{swim} \rangle = U_0^2 \tau_R \left[\left(\frac{1}{6} + \frac{2}{135} (\alpha H_0)^2 \right) + \frac{2\chi_R}{27} \alpha H_0 - \chi_R^2 \left(\frac{7}{135} - \frac{(\alpha H_0)^2}{189} \right) \right] + \mathcal{O}(\chi_R^3), \quad (25)$$

$$\langle D_{\perp}^{swim} \rangle = U_0^2 \tau_R \left[\left(\frac{1}{6} + \frac{1}{90} (\alpha H_0)^2 \right) + \frac{\chi_R}{18} \alpha H_0 - \chi_R^2 \left(\frac{1}{40} - \frac{59(\alpha H_0)^2}{22680} \right) \right] + \mathcal{O}(\chi_R^3). \quad (26)$$

As $\alpha H_0 \rightarrow 0$, the results reduce to the uniform-speed solution considered earlier. The striking feature is that the dispersion *increases* at small χ_R , unlike the uniform-velocity case (compare with Eq 14). Since the swimmers oriented towards the field move faster than those oriented away from the field, we see an enhanced dispersion (and swim stress) at low to intermediate χ_R . As we shall see from the exact solution, the swim stress in both parallel and perpendicular directions continue to increase and reach a maximum at intermediate χ_R .

Another key difference is the anisotropic swim stress at $\chi_R = 0$; the parallel diffusion is larger (2/135 versus 1/90 for $\alpha H_0 = 1$). The average drift velocity from Eq 24 increases the effective translational diffusivity above $U_0^2 \tau_R / 6$ even at $\chi_R = 0$. This drift velocity may help explain the observed migration of bacteria along a temperature gradient.²¹

At high χ_R , the behavior is similar to the uniform-velocity case. Since all particles are oriented along the external field, the effect of swimming-speed nonuniformity becomes negligible and the particles swim in the same direction with the same speed. The swim stress at high χ_R is

$$\sigma^{swim} = -n\zeta U_0^2 \tau_R \left[\frac{1}{2} (1 + 2\alpha H_0)^2 \chi_R^{-3} \hat{\mathbf{H}} \hat{\mathbf{H}} + (1 + \alpha H_0)^2 \chi_R^{-2} (\mathbf{I} - \hat{\mathbf{H}} \hat{\mathbf{H}}) \right]. \quad (27)$$

The swim stress as a function of χ_R for $\alpha H_0 = 1$ is shown in Fig 8A. The instantaneous swimming speed is twice the uniform speed when the swimmer is oriented along the field ($2U_0$) and zero when oriented in the opposite direction. The

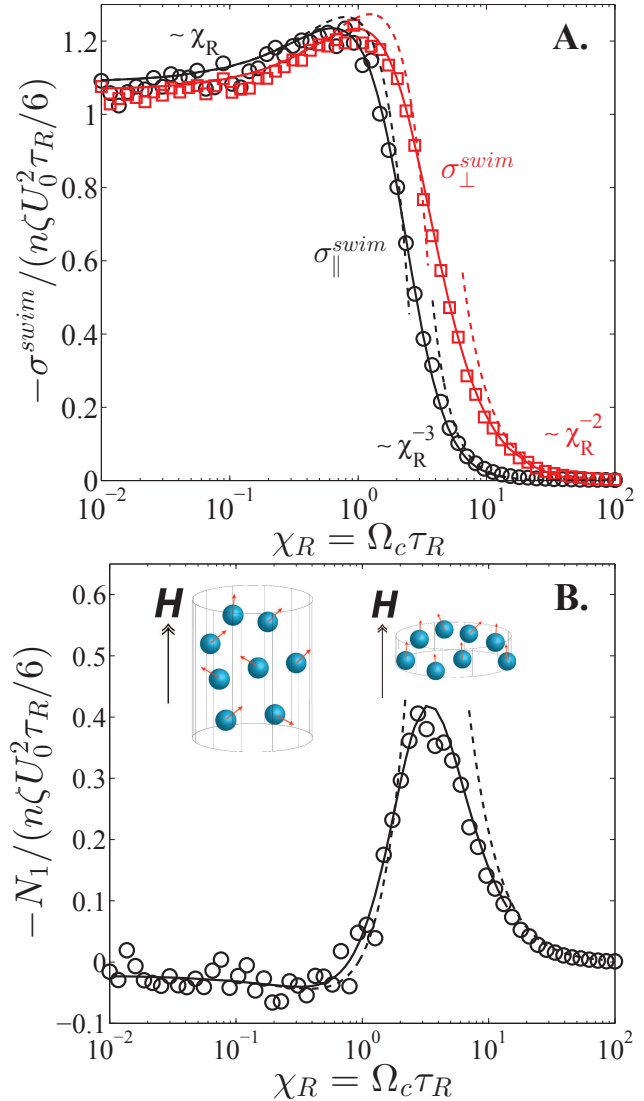


Fig. 8 (A.) Swim stress in the parallel (in black) and perpendicular (in red) directions as a function of χ_R for $\alpha H_0 = 1$. The αH_0 parameter allows the swimming speed to vary with particle orientation. (B.) First normal swim-stress difference. The illustration shows an instantaneous configuration of the swimmers under a weak (sketch on left) and moderate (on right) external field. In both (A) and (B), the solid curves are the exact solutions, and the dashed curves are the asymptotic solutions. BD simulation results are shown in circles and squares for the parallel and perpendicular directions, respectively.

swim stress increases at low to moderate χ_R and reaches a maximum at $\chi_R^{max} = 0.60$ and $\chi_R^{max} = 0.95$ in the parallel and perpendicular directions, respectively. We see maxima because the field redistributes the orientations *and* modifies the swimming speeds. This is different from the uniform-speed case where the field affected only the swimming orientations.

As shown in Fig 8B, the normal swim-stress difference is non-monotonic and also changes in sign from negative to positive at $\chi_R \approx 0.8$.

We saw in Fig 7 that an external field that affects the particles' swimming orientation (but not their speed) resulted in a monotonically decreasing swim pressure with χ_R . As shown in Fig 9, the swim pressure becomes non-monotonic when both the particles' swimming orientation and speed are affected by the external field. This is interesting because an external field can give a non-monotonic pressure profile at the single-particle level (i.e., an infinitely dilute system).

In the Introduction we discussed an important application of loading a soft, compressible gel with active particles. Here we support the description of Fig 1 with our results. When the colloidal particles are inactive, the gel assumes some equilibrium shape as shown on the top of Fig 1. Activating the colloidal particles causes the gel to swell due to the "ideal-gas" swim pressure of the active particles, $\Pi^{swim} = n\zeta U_0^2 \tau_R / 6$. Since the shear modulus of polymer networks can be adjusted over a wide range (in principle to nearly zero) and the intrinsic activity of the swimmers can be made much larger than the thermal energy, $\zeta U_0^2 \tau_R \gg k_B T$, the swim pressure can make an appreciable contribution to the overall size of the gel.

When we then apply a weak external field (i.e., $\chi_R < 1$), the gel expands even more due to increased swim pressures (see Fig 9), elongates due to positive normal stress differences (see Fig 8B), and translates due to the net motion of the active swimmers (see Eq 24) within the gel. When we increase the external field strength ($1 < \chi_R \ll \infty$), the swim pressure decreases and the normal stress difference becomes negative (Fig 8B graphs $-N_1$), which causes the gel to shrink in size, translate faster towards the field direction, and assume the shape of a thin disk as shown to the left of Fig 1. When the external field strength becomes very high ($\chi_R \rightarrow \infty$), the normal swim-stress difference and swim pressure vanish, causing the gel to return to its equilibrium shape and size but translate in the field direction. When the external field is turned off, the gel stops translating and an entire cycle is completed as depicted in Fig 1. Each transformation of the gel is corroborated by our calculations and BD simulations.

Allowing the swimming speeds to vary with orientation introduces features similar to the sedimentation problem considered by Brenner¹⁴ and Almog and Frankel.¹⁵ In the effective translational diffusivity (Eqs 25 and 26), the terms involving $(\alpha H_0)^2$ are identical to those by Almog and Frankel.¹⁵ When analyzing the motion of a single particle, there is no distinction between a motion caused by an external force (i.e., gravity) and a motion arising from intrinsic particle activity (i.e., swim force). Therefore, the perturbation $u' = \alpha H_0 \hat{H} \cdot \mathbf{q}$ in the modified velocity expression is the same as adding a contribution from an external force, $\mathbf{M}(\mathbf{q}) \cdot \mathbf{F}^{ext}$, where $\mathbf{M}(\mathbf{q})$ is the orientation-dependent mobility and \mathbf{F}^{ext} is the external force.

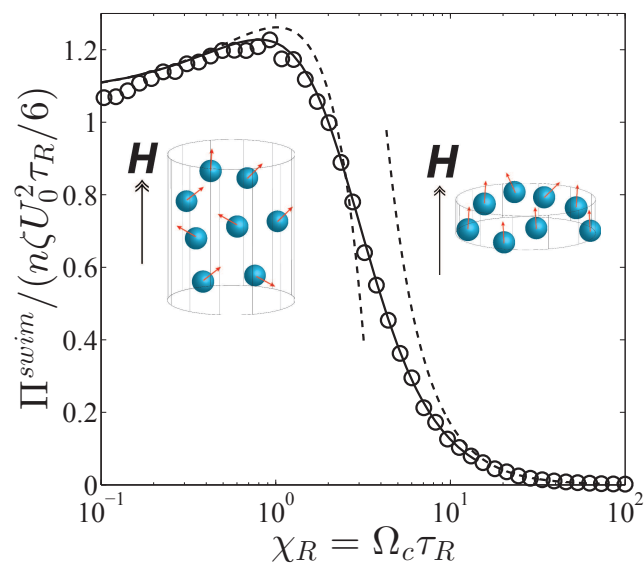


Fig. 9 The swim pressure, $\Pi^{swim} = -\text{tr}\sigma^{swim}/3$, as a function of χ_R for $\alpha H_0 = 1$. The circles are results from BD simulations, and the solid and dashed curves are the exact and asymptotic analytical solutions, respectively. The illustration shows an instantaneous configuration of the swimmers under a weak (sketch on left) and moderate (on right) external field.

Of course, one could assume an expression of $u'(\alpha H_0 \hat{H} \cdot \mathbf{q})$ that is different from the linear relationship (Eq 22) considered here, and the results would no longer be the same as the sedimentation problem. Therefore, the sedimentation problem is a special case of our general formulation.

7 Conclusions

We have introduced a new approach to understand and compute the active stress in a system of self-propelled bodies. All active matter systems generate a unique swim pressure through their intrinsic self-motion. Here we used this swim stress perspective to analyze the effect of an external field on the motion and deformation of active matter. We saw that the external field engendered anisotropic stresses, meaning that the swimmers experience a different confining force in the parallel and perpendicular directions. This lead directly to the shrinking/expanding, elongating, and translating of soft, compressible materials that are loaded with active particles. The external field can thus be used to manipulate the shape and size of soft materials such as a gel or perhaps a biological membrane. Another important application may be the analysis of various biophysical systems, such as the interior of a cell. Molecular motors that activate the cytoskeleton must exert a swim pressure on the cell owing to their self-motion along a track.

Our analysis remains valid for non-spherical particles with a varying swim velocity U_0 and/or reorientation time τ_R . Here we focused on a dilute system of swimmers, but inclusion of two-body effects in the Smoluchowski Eq 1 is straightforward. For non-spherical particles the hydrodynamic drag tensor, ζ , varies with the director \mathbf{q} , and the effective hydrodynamic drag factor $\zeta^{eff} = (2\zeta_{\perp} + \zeta_{\parallel})/3$ becomes the relevant quantity in the stress-diffusivity relationship, where ζ_{\perp} and ζ_{\parallel} are the transverse and parallel components of the hydrodynamic drag tensor, respectively. At finite volume fractions, the particle size, a , would enter in the form of a nondimensional rotary Péclet number, $Pe_R = U_0 a / \langle D^{swim} \rangle \sim a / (U_0 \tau_R)$, which compares the swimmer size a to its run length $U_0 \tau_R$. With the inclusion of translational Brownian motion, all three parameters must be varied in the analysis: $\chi_R = \Omega_c \tau_R$, $Pe_R = a / (U_0 \tau_R)$, and the swim Péclet number $Pe_s = U_0 a / D_0$.

In our analysis we neglected hydrodynamic interactions among the particles, which would contribute additional terms to the active-particle stress and affect the reorientation time of the particles due to translation-rotation coupling. It is important to note that the swim stress is distinct and different from the “hydrodynamic stresslet”, which is also a single-particle property but scales as $\sim n\zeta U_0 a$.^{10,11} As mentioned before, the motion of a single particle due to an intrinsic swim force and an external force are the same. At higher concentrations or when considering the swimmer’s interactions with other bodies or boundaries a distinction must be made—the intrinsic swim mechanism does not generate a long-range $1/r$ Stokes velocity field as does an external force.

Here we focused on a dilute system of active particles, but at higher concentrations active systems have been known to exhibit unique collective behavior.^{1,29} The swim pressure presented here remains valid and appropriate for hydrodynamically interacting active systems, but one needs to carefully examine the individual contributions to the active stress. A single particle hydrodynamic contribution to the stress is of the form $\sim n\zeta a U$, which, while important, is much smaller by a factor of $U_0 \tau_R / a$ than the swim pressure. A complete study would need to consider the effects of both the swim and hydrodynamic stresses. We believe that the experimental, numerical, and theoretical analyses of active systems may need to be revisited in light of the new swim stress concept.

Experimentally, the precise manipulation of colloids using external fields is critical in many applications, like the targeted transport and delivery of specific chemicals.³⁰ Active-matter systems are ideal candidates for understanding dynamic self-assembly and developing synthetic structures. For example, dipolar particles subjected to a magnetic or electric field have been shown to form patterns.^{30–32} Self-assembly and clustering behavior in active matter have been analyzed from the swim stress perspective,² and it would be straightforward to extend these ideas to self-propelled particles that are biased

by an external orienting field.

Acknowledgments

SCT is supported by the Gates Millennium Scholars fellowship and the National Science Foundation Graduate Research Fellowship under Grant No. DGE-1144469.

Appendix

A: Low- χ_R limit

A regular perturbation expansion of Eqs 11 and 12 assumes solutions of the form $g_0(\mathbf{q}; \chi_R) = g_0^{(0)}(\mathbf{q}) + g_0^{(1)}(\mathbf{q})\chi_R + g_0^{(2)}(\mathbf{q})\chi_R^2 + \mathcal{O}(\chi_R^3)$ and $\mathbf{d}(\mathbf{q}; \chi_R) = \mathbf{d}^{(0)}(\mathbf{q}) + \mathbf{d}^{(1)}(\mathbf{q})\chi_R + \mathbf{d}^{(2)}(\mathbf{q})\chi_R^2 + \mathcal{O}(\chi_R^3)$.

Substituting these into Eq 11 of the text, the leading-order orientation distribution function $g_0^{(0)}$ satisfies $\nabla_q^2 g_0^{(0)} = 0$ and $\oint g_0^{(0)} d\mathbf{q} = 1$. The solution is the uniform distribution, $g_0^{(0)} = 1/4\pi$. The $\mathcal{O}(\chi_R)$ problem is $-\hat{\mathbf{H}} \cdot \mathbf{q} / (2\pi) = \nabla_q^2 g_0^{(1)}$ with $\oint g_0^{(1)} d\mathbf{q} = 0$. From Brenner²⁷, vector spherical surface harmonics satisfy

$$\nabla_q^2 \mathbf{P}_n(\mathbf{q}) = -n(n+1)\mathbf{P}_n(\mathbf{q}). \quad (\text{A1})$$

We hence substitute the trial solution $g_0^{(1)} = \mathbf{P}_1(\mathbf{q}) \cdot \mathbf{a}_1$ into Eq A1, and obtain $\mathbf{a}_1 = \hat{\mathbf{H}}/4\pi$. Thus, the solution is $g_0^{(1)} = \hat{\mathbf{H}} \cdot \mathbf{P}_1(\mathbf{q}) / (4\pi)$. The $\mathcal{O}(\chi_R^2)$ problem is solved similarly: $\nabla_q^2 g_0^{(2)} = -\hat{\mathbf{H}}\hat{\mathbf{H}} : \mathbf{P}_2(\mathbf{q}) / (2\pi)$ with $\oint g_0^{(2)} d\mathbf{q} = 0$. The solution is $g_0^{(2)} = \hat{\mathbf{H}}\hat{\mathbf{H}} : \mathbf{P}_2(\mathbf{q}) / (12\pi)$. Substitution of these three contributions into the perturbation expansion, we arrive at the solution in the text.

A similar procedure for the \mathbf{d} -field gives

$$\mathbf{d} = -\frac{1}{8\pi} \mathbf{P}_1(\mathbf{q}) - \frac{5\chi_R}{72\pi} \hat{\mathbf{H}} \cdot \mathbf{P}_2(\mathbf{q}) + \frac{\chi_R^2}{\pi} \left(\frac{29}{1440} \hat{\mathbf{H}}\hat{\mathbf{H}} \cdot \mathbf{P}_1(\mathbf{q}) - \frac{13}{720} \hat{\mathbf{H}}\hat{\mathbf{H}} : \mathbf{P}_3(\mathbf{q}) - \frac{3}{160} \mathbf{P}_1(\mathbf{q}) \right) + \mathcal{O}(\chi_R^3). \quad (\text{A2})$$

As in the force-induced microrheology problem considered by Zia and Brady²³, the $\mathcal{O}(1)$ solution for \mathbf{d} is the same as the $\mathcal{O}(\chi_R)$ problem for g_0 . In the linear-response regime, the problems are identical whether the swimmers are reoriented by the external field (g_0) or by thermal energy $k_B T$ (\mathbf{d}) and the same holds true when the reorientation is athermal with τ_R .

B: High- χ_R limit

The problem is singular in the $\chi_R \gg 1$ limit, so we expand the solution in the inner region as $g_0(\hat{\mu}; \chi_R) = \chi_R g_0^{(0)}(\hat{\mu}) +$

$g_0^{(1)}(\hat{\mu}) + \mathcal{O}(\chi_R^{-1})$. Substituting into Eq 11 of the text, the leading-order solution satisfies

$$\frac{d}{d\hat{\mu}} \left[\hat{\mu} \left(g_0^{(0)} + \frac{dg_0^{(0)}}{d\hat{\mu}} \right) \right] = 0, \quad (\text{B1})$$

with $\int_0^{2\pi} \int_0^\infty g_0^{(0)}(\hat{\mu}) d\hat{\mu} d\phi = 1$. For the fluctuation field, we separate the solution into scalar components parallel and perpendicular to $\hat{\mathbf{H}}$ as $\mathbf{d}(\mu, \phi; \chi_R) = d_{\parallel}(\mu; \chi_R)\hat{\mathbf{H}} + d_{\perp}(\mu; \chi_R)(\mathbf{e}_x \cos \phi + \mathbf{e}_y \sin \phi)$, where \mathbf{e}_x and \mathbf{e}_y are unit vectors in the x and y directions, respectively (see Fig 3). We assume subject to posteriori verification that d_{\parallel} and d_{\perp} are only a function of μ . Substituting the scaled $\hat{\mu}$ variable into Eq 12, we obtain

$$\frac{d}{d\hat{\mu}} \left[\hat{\mu} \left(d_{\parallel} + \frac{dd_{\parallel}}{d\hat{\mu}} \right) \right] = -\frac{1}{4\pi} e^{-\hat{\mu}} \chi_R^{-1} (\hat{\mu} - 1), \quad (\text{B2})$$

$$\frac{d}{d\hat{\mu}} \left[\hat{\mu} \left(d_{\perp} + \frac{dd_{\perp}}{d\hat{\mu}} \right) \right] - \frac{d_{\perp}}{4\hat{\mu}} = \frac{\sqrt{2}}{4\pi} \chi_R^{-1/2} e^{-\hat{\mu}} \hat{\mu}^{1/2}. \quad (\text{B3})$$

The leading nonzero solution is of order $d_{\parallel} \sim \mathcal{O}(\chi_R^{-1})$ and $d_{\perp} \sim \mathcal{O}(\chi_R^{-1/2})$. In the parallel direction, the solution is $d_{\parallel}(\hat{\mu}; \chi_R) = \chi_R^{-1} e^{-\hat{\mu}} (\hat{\mu} - 1)/(4\pi) + \mathcal{O}(\chi_R^{-2})$, which satisfies both the regularity and normalization conditions. In the perpendicular direction, we obtain $d_{\perp}(\hat{\mu}; \chi_R) = -\chi_R^{-1/2} \hat{\mu}^{1/2} e^{-\hat{\mu}}/(\sqrt{2}\pi) + \mathcal{O}(\chi_R^{-1})$. Using boundary-layer coordinates, the effective translational diffusivity is computed from

$$\langle \mathbf{D} \rangle - \mathbf{D}_0 = \langle \mathbf{D}^{swim} \rangle = \pi U_0^2 \tau_R \int_0^\infty \left[2\chi_R^{-2} (1 - \hat{\mu}) d_{\parallel} \hat{\mathbf{H}} \hat{\mathbf{H}} + \sqrt{2}\chi_R^{-3/2} d_{\perp} \hat{\mu}^{1/2} (\mathbf{I} - \hat{\mathbf{H}} \hat{\mathbf{H}}) \right] d\hat{\mu}. \quad (\text{B4})$$

C: Exact solution for arbitrary χ_R : Uniform speeds

We rewrite Eq 11 as

$$\frac{d}{d\mu} \left[(1 - \mu^2) \frac{dg_0}{d\mu} \right] - \chi_R \frac{d}{d\mu} [(1 - \mu^2)g_0] = 0, \quad (\text{C1})$$

where $\mu \equiv \hat{\mathbf{H}} \cdot \mathbf{q}$. Twice integrating and invoking the normalization and regularity conditions (finite $dg_0/d\mu$ and g_0 at $\mu = \pm 1$), we arrive at Eq 16 of the text. The corresponding displacement field is broken into the parallel and perpendicular components. The solution in the parallel direction is

$$d_{\parallel}(\mu; \chi_R) = \frac{e^{\mu\chi_R}}{8\pi(\sinh \chi_R)^2} \left[\cosh(\chi_R) \log \left(\frac{1 - \mu}{1 + \mu} \right) - \sinh(\chi_R) \log(1 - \mu^2) + e^{\chi_R} Ei(-\chi_R(\mu + 1)) - e^{-\chi_R} Ei(\chi_R(1 - \mu)) \right] + A_{\parallel} e^{\mu\chi_R}, \quad (\text{C2})$$

where $Ei(t)$ is the exponential integral $Ei(t) \equiv \int_{-\infty}^t e^{-\zeta}/\zeta d\zeta$, and A_{\parallel} is the normalization constant:

$$A_{\parallel} = -\frac{\chi_R}{16\pi(\sinh \chi_R)^3} \int_{-1}^1 e^{\mu\chi_R} \left[\cosh(\chi_R) \log \left(\frac{1 - \mu}{1 + \mu} \right) - \sinh(\chi_R) \log(1 - \mu^2) + e^{\chi_R} Ei(-\chi_R(\mu + 1)) - e^{-\chi_R} Ei(\chi_R(1 - \mu)) \right] d\mu. \quad (\text{C3})$$

In the perpendicular direction, the solution is expanded as $d_{\perp} = \sum_{n=1}^{\infty} C_n P_n^1(\mu)$. The coefficients C_n are found by solving a tridiagonal matrix problem:

$$-\chi_R \frac{(n+1)(n-1)}{2n-1} C_{n-1} + n(n+1)C_n + \chi_R \frac{n(n+2)}{2n+3} C_{n+1} = b_n, \quad (\text{C4})$$

with $C_0 = C_{N+1} = 0$, and the forcing coefficients b_n are given by

$$b_n = -\frac{2n+1}{2n(n+1)} \int_{-1}^1 g_0(\mu; \chi_R) \sqrt{1 - \mu^2} P_n^1 d\mu. \quad (\text{C5})$$

From Eq 9, the swim diffusivity and stress are

$$\sigma^{swim} = -n\zeta \langle \mathbf{D}^{swim} \rangle = -n\zeta U_0^2 \tau_R \pi \int_{-1}^1 \left[2d_{\parallel} (\coth \chi_R - \chi_R^{-1} - \mu) \hat{\mathbf{H}} \hat{\mathbf{H}} + d_{\perp} \sqrt{1 - \mu^2} (\mathbf{I} - \hat{\mathbf{H}} \hat{\mathbf{H}}) \right] d\mu, \quad (\text{C6})$$

where only the symmetric terms contribute to the quadrature. In the perpendicular direction, the convenience of using associated Legendre polynomials is evident in

$$\sigma_{\perp}^{swim} = -n\zeta U_0^2 \tau_R \pi \int_{-1}^1 \sum_{n=1}^{\infty} C_n P_n^1(\mu) P_1^1(\mu) d\mu = -\frac{4\pi}{3} n\zeta U_0^2 \tau_R C_1. \quad (\text{C7})$$

D: Exact solution for arbitrary χ_R : Nonuniform speeds

Resolving Eq 19 into the parallel and perpendicular components, the exact \mathbf{d} -field solution in the parallel direction is

$$d_{\parallel} = \frac{e^{\mu\chi_R}}{8\pi(\sinh \chi_R)^2} \left\{ \left(1 - \frac{2\alpha H_0}{\chi_R} \right) \left[\cosh(\chi_R) \log \left(\frac{1 - \mu}{1 + \mu} \right) - \sinh(\chi_R) \log(1 - \mu^2) + e^{\chi_R} Ei(-\chi_R(\mu + 1)) - e^{-\chi_R} Ei(\chi_R(1 - \mu)) \right] - 2\alpha H_0 \mu \sinh \chi_R \right\} + \tilde{A}_{\parallel} e^{\mu\chi_R}, \quad (\text{D1})$$

where \tilde{A}_{\parallel} is found from the normalization constraint to be

$$\tilde{A}_{\parallel} = -\frac{\chi_R}{16\pi(\sinh \chi_R)^3} \int_{-1}^1 e^{\mu\chi_R} \left\{ \left(1 - \frac{2\alpha H_0}{\chi_R}\right) \times \left[\cosh(\chi_R) \log\left(\frac{1-\mu}{1+\mu}\right) - \sinh(\chi_R) \log(1-\mu^2) + e^{\chi_R} Ei(-\chi_R(\mu+1)) - e^{-\chi_R} Ei(\chi_R(1-\mu)) \right] - 2\alpha H_0 \mu \sinh \chi_R \right\} d\mu. \quad (\text{D2})$$

Substitution of this equation into Eq 9 gives the swim stress in the parallel direction.

In the perpendicular direction, the form of the solution is the same as before (Eq C4) except the forcing coefficients b_n are given by

$$b_n = -\frac{2n+1}{2n(n+1)} \int_{-1}^1 g_0(\mu; \chi_R) \sqrt{1-\mu^2} (1 + \alpha H_0 \mu) P_n^1 d\mu. \quad (\text{D3})$$

The tridiagonal matrix problem is solved for the coefficients C_{n-1} , C_n , and C_{n+1} . The effective translational diffusivity in the perpendicular direction is given by

$$\langle D_{\perp} \rangle = 4\pi U_0^2 \tau_R \left(\frac{1}{3} C_1 + \frac{1}{5} \alpha H_0 C_2 \right), \quad (\text{D4})$$

where we have used the orthogonality of the associated Legendre functions $P_1^1 = -\sqrt{1-\mu^2}$ and $P_2^1 = -3\mu\sqrt{1-\mu^2}$ to evaluate the integral.

References

- 1 S. Ramaswamy, *Ann Rev Condens Matter Phys*, 2010, **1**, 323–345.
- 2 S. C. Takatori, W. Yan and J. F. Brady, *Phys Rev Lett*, 2014, **113**, 028103.
- 3 J. Adler, *Science*, 1966, **153**, 708–716.
- 4 J. Armitage and K. Hellingwerf, *Photosynth Res*, 2003, **76**, 145–155.
- 5 R. Blakemore, *Science*, 1975, **190**, 377–379.
- 6 D. Hader, R. Hemmersbach and M. Lebert, *Gravity and the Behavior of Unicellular Organisms*, Cambridge University Press, Cambridge, United Kingdom, 2005.
- 7 M. Doi, *Soft Matter Physics*, Oxford University Press, Oxford, United Kingdom, 2013.
- 8 D. S. Fudge, T. Winegard, R. H. Ewoldt, D. Beriault, L. Szewciw and G. H. McKinley, *Integrative and comparative biology*, 2009, **49**, 32–39.
- 9 S. K. Lai, Y.-Y. Wang, D. Wirtz and J. Hanes, *Adv Drug Deliv Rev*, 2009, **61**, 86–100.
- 10 D. Saintillan and M. J. Shelley, *Phys Fluids*, 2008, **20**, 123304–123315.
- 11 T. Ishikawa, M. P. Simmonds and T. J. Pedley, *J Fluid Mech*, 2006, **568**, 119–160.
- 12 I. Theurkauff, C. Cottin-Bizonne, J. Palacci, C. Ybert and L. Bocquet, *Phys Rev Lett*, 2012, **108**, 268303.
- 13 J. Palacci, S. Sacanna, A. P. Steinberg, D. J. Pine and P. M. Chaikin, *Science*, 2013, **339**, 936–940.
- 14 H. Brenner, *J Colloid Interface Sci*, 1979, **71**, 189–208.

- 15 Y. Almog and I. Frankel, *J Colloid Interface Sci*, 1993, **157**, 60–71.
- 16 M. A. Bees, N. A. Hill and T. J. Pedley, *J Math Biol*, 1998, **36**, 269–298.
- 17 A. Manela and I. Frankel, *J Fluid Mech*, 2003, **490**, 99–127.
- 18 T. J. Pedley and J. O. Kessler, *J Fluid Mech*, 1990, **212**, 155–182.
- 19 R. N. Bearon, A. L. Hazel and G. J. Thorn, *J Fluid Mech*, 2011, **680**, 602–635.
- 20 R. N. Bearon, M. A. Bees and O. A. Croze, *Phys Fluids*, 2012, **24**, 121902–121920.
- 21 M. Demir and H. Salman, *Biophys J*, 2012, **103**, 1683–1690.
- 22 R. R. Vuppula, M. S. Tirumkudulu and K. V. Venkatesh, *Phys Biol*, 2010, **7**, 026007.
- 23 R. N. Zia and J. F. Brady, *J Fluid Mech*, 2010, **658**, 188–210.
- 24 U. M. Córdova-Figueroa and J. F. Brady, *Phys Rev Lett*, 2008, **100**, 158303.
- 25 H. Brenner and D. Edwards, *Macrotransport Processes*, Butterworth-Heinemann Limited, 1993.
- 26 H. Brenner and D. W. Condiff, *J Colloid Interface Sci*, 1974, **47**, 199–264.
- 27 H. Brenner, *Chem Engng Sci*, 1964, **19**, 631–651.
- 28 D. A. Beard and T. Schlick, *Biophys J*, 2003, **85**, 2973–2976.
- 29 J. Toner, Y. Tu and S. Ramaswamy, *Ann Phys*, 2005, **318**, 170–244.
- 30 A. Snezhko and I. S. Aranson, *Nat Mater*, 2011, **10**, 698–703.
- 31 M. V. Sapozhnikov, Y. V. Tolmachev, I. S. Aranson and W. K. Kwok, *Phys Rev Lett*, 2003, **90**, 114301.
- 32 M. E. Leunissen, H. R. Vutukuri and A. van Blaaderen, *Adv Mater*, 2009, **21**, 3116–3120.

Table of contents entry

Manuscript ID: SM-ART-06-2014-001409

Title: Swim Stress, Motion, and Deformation of Active Matter: Effect of an External Field

Authors: S.C. Takatori, J.F. Brady

Abstract text: We analyze the stress, dispersion, and average swimming speed of self-propelled particles subjected to an external field, and discuss a method to manipulate soft compressible materials as nano/micromechanical devices and motors.

Color graphic. Please use Figure 1 in our main text:

